

Analysis, purification, and characterization of peroxidases in rosemary using chromatography and spectrometry techniques

Noor Hatem Jumaa^{a,*}, Sara Thualfuqar Jamil^a, Hajir Hilal^a, Mukaram Shikara^a, Ahmed Abd Temur^b,
Ameerah Hussein Qader^a, Zinah Hilal Khaleel^c, and Doha Khalil Ibrahim^a

^aDepartment of Medical Laboratory Techniques, College of Health and Medical Techniques, Al-Esraa University, Baghdad, Iraq

^bDepartment of Applied Pathological Analysis, College of Science, Al-Nahrain University, Baghdad, Iraq

^cCollege of Pharmacy, Al-Esraa University, Baghdad, Iraq

ARTICLE INFO:

Received 7 Jul 2025

Revised form 9 Sep 2025

Accepted 22 Oct 2025

Available online 25 Dec 2025

Keywords:

Rosemary peroxidase,
Chromatographic techniques,
High-performance liquid
chromatography,
Atomic absorption spectrometry,
Purification,
Enzyme activity

ABSTRACT

Rosemary (*Salvia Rosmarinus*) peroxidase was purified by chromatographic techniques, yielding an enzyme recovery of 35%. The estimated molecular mass was 47 kDa, determined by Sodium Dodecyl Sulfate-Polyacrylamide Gel Electrophoresis (SDS-PAGE), and it has an isoelectric focusing point at 4.33. The optimal pH and temperature were 6.0 and 40°C, respectively. Michaelis constant (Km) values were 3.7 mg mL⁻¹, and the specific activity (SA) values were 28.10 U min⁻¹ mL⁻¹ towards guaiacol. The purified peroxidase activity was increased with calcium, ferric, magnesium, and manganese ions but decreased with copper, mercury, and zinc ions at all tested concentrations. The data indicate that this enzyme is a promising source of industrial peroxidase. Flame atomic absorption spectrometry (FAAS) was used to detect metals in rosemary. To validate peroxidase levels in rosemary using high-performance liquid chromatography (HPLC), we would typically extract the enzyme, purify it (ammonium sulfate), and then separate and quantify it using an HPLC-UV method. The method usually involves using a C18 column and UV detection, with specific wavelengths chosen based on the peroxidase products. The mean LOD and LOQ methods, based on microgram injections, were determined to be 0.051 and 0.153 µg mL⁻¹, respectively, using the standard deviation of blank peak areas from 10 blank samples (RSD% < 4%). The rosemary extract is injected into the HPLC, and the calibration curve identifies the peroxidase peak.

1. Introduction

Biological roles in rosemary include detoxifying hydrogen peroxide, lignin formation, phenolic compound oxidation, and contributions to flavor and aroma stability during storage. Rosemary peroxidases exhibit activity towards certain chemicals, including guaiacol, pyrogallol, o-dianisidine, and 2,2'-azino-bis (3-ethylbenzothiazoline-6-sulfonic acid) (ABTS).

Isoforms of rosemary have molecular weights ranging from 30 to 70 kDa, depending on the isoform. Their isoelectric points (pI) range from 3.5 to 9.0. The optimum activity of rosemary peroxidases occurs at pH 5–7, with a temperature optimum between 30 and 50 °C. Peroxidase types in rosemary include Guaiacol peroxidases, which catalyze the oxidation of guaiacol to tetraguaiacol (brown pigment). Ascorbate peroxidases (APX) use ascorbic acid as the electron donor and play a role in scavenging reactive oxygen species (ROS) in plant tissues. Also, peroxidases in rosemary include phenolic peroxidases (which

*Corresponding Author: Noor Hatem Jumaa

Email: noorhatim8@gmail.com

<https://doi.org/10.24200/amecj.v8.i04.1090>

oxidize phenolic compounds, such as caffeic acid and rosmarinic acid) and lignin peroxidases. Rosemary (*Salvia rosmarinus*) is one of the hundreds of species in the genus *Salvia* (family Lamiaceae), which are distributed across a large area of the Middle East. They grow as annual or perennial herbaceous plants, rarely as shrubs, reaching 1.2–1.8 meters in height [1]. Some people use the whole plant for herbal tea, while others use it as animal fodder. However, it can also be an excellent source of industrially produced peroxidases. Peroxidases (Peroxide reductases EC 1.11.1.X) are heme-containing enzymes generally found in species that catalyze the redox reactions of a broad diversity of phenol compounds, as well as non-phenol compounds, by using H_2O_2 [2,3]. Plants' peroxidases belong to class III and participate in a broad diversity of activities such as hormone catabolism, auxin metabolism, ethylene biosynthesis, ripening of fruits, lignin polymerization, senescence, suberization, H_2O_2 generation, toxins' oxidations, lignin biosynthesis, reactions to plants stresses (ex., wounds or attacks), and many other functions [4-7]. Peroxidases were extracted, purified, and characterized from a variety of plants such as seeds of apples and oranges, artichoke (*Cynara scolymus* L.), *C. sinensis*, Date fruits, garlic, guinea grass, horseradish, *M. oleifera*, manioc (*Manihot utilissima*), *N. tabacum*, peach (*Prunus persica*), radish, potato (*Solanum tuberosum*), tomato, yam (*Alocasia macrorrhiza*), and zucchini (*Cucurbita pepo*) [8,9]. With modern biotechnology, peroxidases, due to their versatile reactions, have potential applications across the medical, nutrition, and other industries. They were used as immunoassay kits due to their ability to catalyze reactions under mild temperature and pH conditions, with broad substrate specificity. These properties made them useful in various applications, including the food industry, bleaching of synthetic dyes, detoxification, and decolorization of wastewater, among others [2, 10-14]. Additionally, other chromatography methods, such as GC-MS and GC-FID, were used to detect organic materials. Flame Atomic Absorption Spectroscopy (F-AAS) and Electrothermal Atomic Absorption Spectroscopy (ETAAS), also known as Graphite Furnace AAS,

were also used for metal analysis [15-25]. GC (GC-MS or GC-FID) is applicable for analyzing small-molecule substrates, oxidation products, and volatile metabolites produced or consumed by rosemary peroxidase activity. GC with Indirect detection was used to measure substrates or products of peroxidase reactions (e.g., phenolic oxidation products, volatile organic compounds, aldehydes). Volatile profiling was used to monitor changes in rosemary essential oils and volatiles after enzyme treatment, and headspace-GC or SPME-GC-MS was used to analyze the samples. Metabolite analysis was performed after enzymatic reaction using GC-MS or GC-FID.

In this study, the Purification and characterization of Rosemary peroxidases were studied. A purified peroxidase from rosemary was used, and SDS-PAGE was employed to determine its molecular mass. The enzyme, molecules, and other compounds in Rosemary peroxidase were separated based on electrical charge using ion-exchange chromatography (IEC) and by molecular size using size-exclusion chromatography (SEC) before analysis by High-Performance Liquid Chromatography (HPLC).

2. Materials and Methods

2.1. Reagents and Instrumental

Fresh, mature Rosemary plants were sourced from local markets in Baghdad, Iraq, between April and June 2021. Analytical-grade reagents and chemicals were obtained from Sigma-Aldrich. HNO_3 (CAS Number: 7697-37-2), H_2SO_4 (CAS Number: 7664-93-9), H_2O_2 (CAS Number: 7722-84-1), $(NH_4)_2SO_4$ (CAS Number: 7783-20-2), McIlvaine buffer (CAS Number: 77-92-9, mixture of citric acid and disodium phosphate for pH between 2.2 and 8.0), glycerol ($C_4H_8O_3$, CAS Number: 99569-11-6, MW: 104), phenylmethylsulphonyl fluoride (PMSF, CAS Number: 329-98-6), NaCl (CAS Number: 7647-14-5), $ZnCl_2$ (CAS Number: 7646-85-7), and ammonium acetate purchased from Sigma, Germany. Chromatographic techniques are essential for enzyme recovery and purification, relying on differences in properties like size, charge, and binding affinity to separate enzymes from complex mixtures. Standard methods

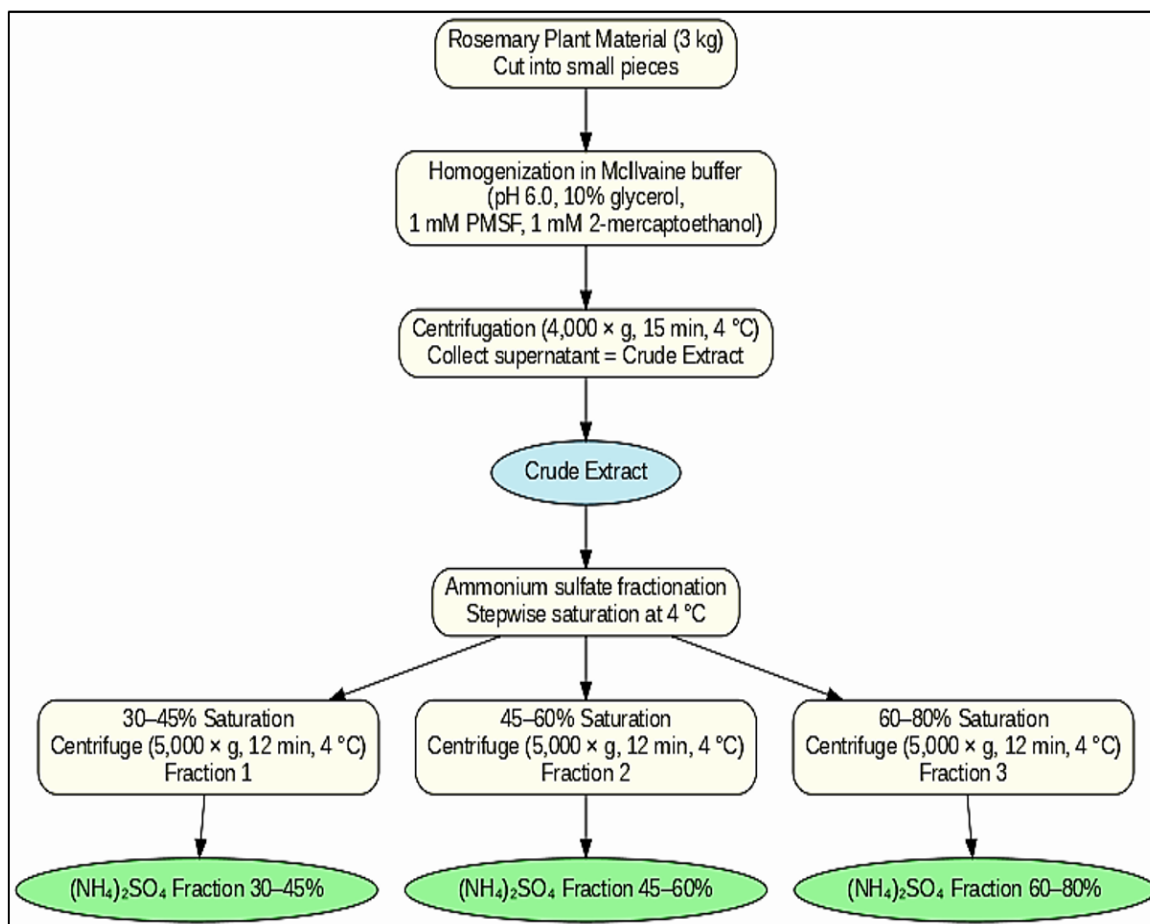
include ion exchange and size exclusion coupled with HPLC. Ion Exchange Chromatography (IEC, Thermo Fisher, USA) separates molecules based on charge differences between the enzyme and other compounds. IEC is a commonly used platform for purifying biologics. Size Exclusion Chromatography (SEC, Agilent), also known as Gel Filtration, separates molecules by size, allowing larger molecules such as enzymes to elute more quickly. Bio SEC-5 HPLC size exclusion chromatography (SEC, Agilent, USA) columns are packed with 5.0 μm silica particles coated with a proprietary, neutral, hydrophilic layer for optimal efficiency and stability.

2.2. Purification of the peroxidase

The purification of Rosemary's peroxidase followed the modified procedure described by Smith and Wilcox (Smith and Wilcox 1970) All operations were carried out at 4°C.

2.2.1. Crude extract and $(\text{NH}_4)_2\text{SO}_4$ fractions step

The whole plants (3.0 kg) were cut into small pieces and suspended in cold McIlvaine buffer (pH 6.0) containing 10% (v/v) glycerol, 1.0 mM phenylmethylsulfonyl fluoride (PMSF) and 1.0 mM 2-mercaptoethanol. Plant material was homogenized in an ice-cold Waring blender for 10 min. The homogenate was centrifuged at $4,000 \times g$ for 15 min at 4 °C, and the supernatant was collected as the crude extract (Schema 1). Ammonium sulfate $[(\text{NH}_4)_2\text{SO}_4]$ fractionation was carried out at 4 °C by stepwise addition of solid $(\text{NH}_4)_2\text{SO}_4$ to reach 30–45%, 45–60% and 60–80% saturation, respectively. After each salt addition the mixture was stirred on ice for 15–30 min and then allowed to equilibrate for a further 30 min before centrifugation at $5,000 \times g$ for 12 min at 4 °C. Pellets from each saturation cut were collected, resuspended in a minimal volume of the above McIlvaine buffer, and desalted by dialysis against



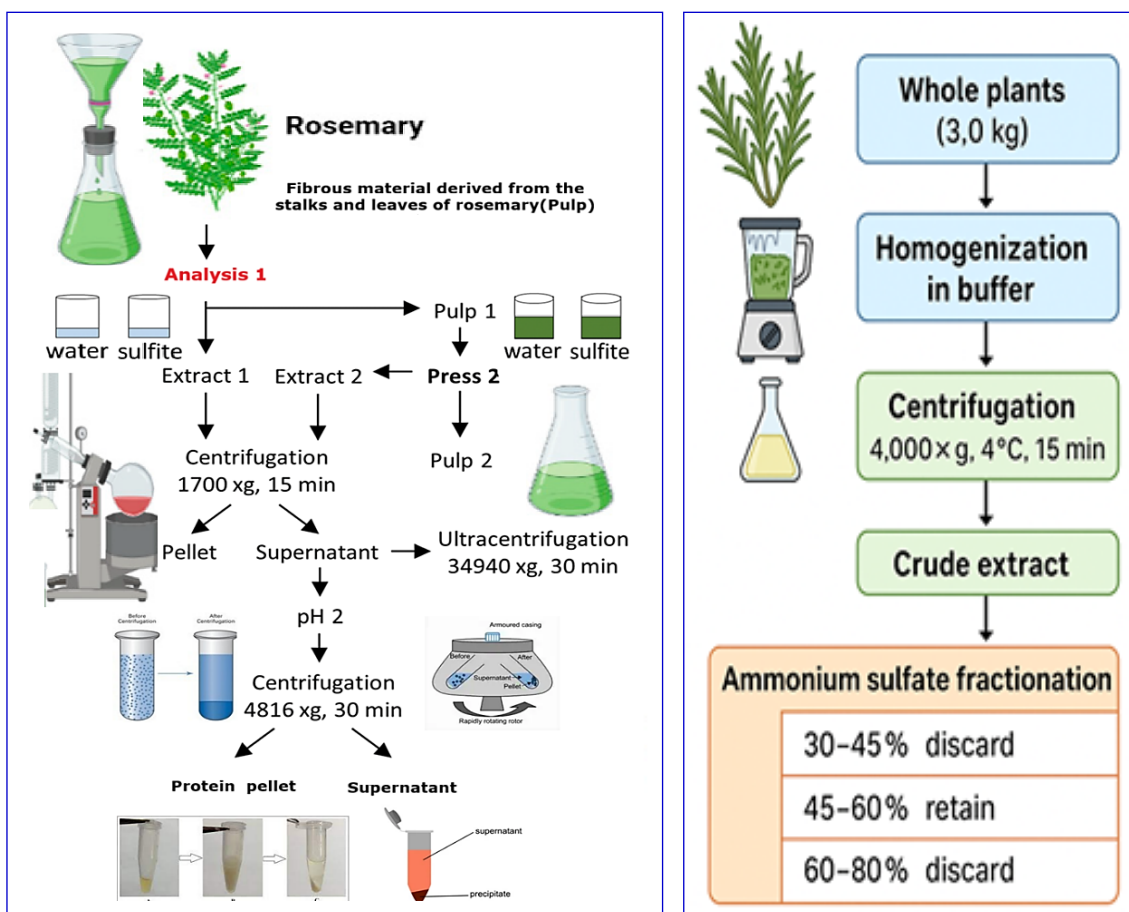
Schema 1. Crude extract and $(\text{NH}_4)_2\text{SO}_4$ fractions step for Rosemary

the same buffer for 12 h with two buffer changes. Desalted fractions were assayed for peroxidase activity (guaiacol/H₂O₂ method) and total protein (Bradford assay). Fractions showing significant peroxidase activity were pooled and kept on ice for subsequent chromatographic purification. A high peroxidase activity was related to the 0.6-0.8% (NH₄)₂SO₄ fraction, so it was used for further purification after it was concentrated by filtration through a collodion bag to about 3.0 mL. The ammonium sulfate fractionation workflows, peroxidase extraction, or protein purification from whole plant material are presented in [Schema 2](#).

2.3. Chromatography and HPLC Analysis

The 0.6-0.8% (NH₄)₂SO₄ fraction was loaded onto a 1.5 × 30 cm phosphocellulose column that had been previously washed with two column volumes of McIlvaine buffer at pH 6.0 (containing 10% glycerol, 1.0 mM phenylmethylsulfonyl

fluoride (PMSF), and 1.0 mM mercaptoethanol). A peroxidase activity was eluted with 80 mL of 0-0.6M NaCl in the McIlvaine buffer, and fractions (3.0 mL) were collected. One-third of each fraction was reserved for further analysis, and the peak fractions were pooled together. Zinc chloride (ZnCl₂) was then added to precipitate any contaminating ribonucleases (RNases) attached to the enzyme. The peak fraction was loaded onto a 1.5 × 15 cm DEAE-cellulose column, pH 6.0, which had been previously washed with McIlvaine buffer. The peroxidase activity was then eluted with 50 mL of 0-0.4M NaCl in the same buffer, and fractions (2.0 mL) were collected. Two-thirds of each fraction were pooled, and the peak fractions were re-chromatographed on 1.5 × 10 cm Sephadex G-100 to remove salts. The peaked fractions were collected and layered into a Matrix gel red-A column (1.5 × 10cm) equilibrated with the same buffer. The peroxidase was eluted with a 0 to 0.4 M sodium



Schema 2. The crude extract based on ammonium sulfate fractionation, including the extract protein pellet and the supernatant of rosemary.

chloride gradient in the same buffer. The peak fractions with the highest peroxidase activity were eluted at approximately 0.14 M sodium chloride. They were pooled, dialyzed, and concentrated (as before), and the resulting preparation was considered purified peroxidase and used for further studies. Protein and carbohydrate concentrations were determined for all fractions.

Additionally, HPLC is used in validation methodologies. The C18 column is a common choice for HPLC separation of plant compounds. Gradient elution with two solvents (methanol/water) is often used to separate compounds. The concentration of peroxidase in the rosemary was determined from the peak area and the calibration curve. Specific wavelengths are chosen based on the peroxidase and the compounds it interacts with (e.g., 280 nm for some phenolic compounds, or 254 nm for rosmarinic acid). Tests such as resolution, peak symmetry, and retention time are checked to ensure the system is functioning correctly. A calibration curve is created using the standard solution to relate peak area to concentration. The rosemary extract is injected into the HPLC, and the peak corresponding to the peroxidase (or its reaction product) is identified and quantified using the calibration curve. Use temperatures of 0–4 °C for all analyses, with buffers free of strong detergents or organic compounds. Desalt the final ammonium sulfate fractions using an HPLC-based method, employing a PD-10 desalting column. Filter through a 0.22 µm PVDF/nylon syringe filter immediately before injection to protect the column. If the sample protein concentration is low, concentrate using ultrafiltration (10 kDa) to achieve ~0.5–2 mg mL⁻¹ for analytical injections, or higher for preparative runs. First, we use ion exchange, either an anion or a cation. Use an anion exchanger if peroxidases are acidic at your chosen pH; use a cation exchanger if peroxidase doesn't bind at neutral pH (Mobile phase of 20 mM sodium phosphate pH 6.5, Flow rate of 0.5 mL min⁻¹, Injection of 20–50 µL and gradient of 0% → 30% in 20 min and 30% → 100% in 5 min). Then, Size-exclusion HPLC (SEC) was used to determine the

oligomeric state and to remove small contaminants while maintaining the enzyme's native structure. Mobile phase of 50 mM sodium phosphate, 150 mM NaCl, pH 7.0; Flow rate of 0.5–0.8 mL min⁻¹; injection: 50–200 µL. The phosphate buffer is used for enzyme stability. If compatibility is needed later, switch to ammonium acetate (50 mM) and reduce the ionic strength. Then adjust the gradient with a 0.5 M ammonium acetate eluent. If nothing binds at pH 6.5, try lowering the pH to 5.0 (for anion exchange, some proteins bind better at slightly lower pH levels) or switch to cation exchange at pH 5.0. Dual-wavelength monitoring simultaneously records A₂₈₀ (protein) and 410 nm (heme Soret). For analysis, you can estimate concentration from A₄₁₀ (A₄₀₈–A₄₁₄) using Beer-Lambert: C (µM) = A / (ε × pathlength). The ε of Rosmary peroxidases is ≈ 162 mM⁻¹ cm⁻¹.

2.3.1. The assay for peroxidase

This assay is a variation of the method by Aydin et al., and OD changes were measured at 480nm [26]. First, 50 µL of the purified peroxidase was added to 1.9 mL of McIlvaine buffer containing 1 mL of H₂O₂ solution (8.8 mM) and 1 mL of 45 mM guaiacol as substrates at pH 6.0 and 40 °C. Units of activity were calculated according to the following empirical formula (Eq. 1). One unit of peroxidase activity was defined as the amount of enzyme that catalyzes the production of 1 mmol of guaiacol per minute [27].

$$\text{units/ml} = \frac{\text{AOD/ min} \times \text{dilution factor} \times 1,000}{\text{ml of enzyme used in the assay}}$$

(Eq.1)

2.4. Protein Analysis

Protein concentrations were measured according to Lowry et al. [28].

2.4.1. SDS-Polyacrylamide Gel Electrophoresis

Sodium dodecyl sulphate (SDS)-PAGE was used for the determination of the molecular weight (MW) of peroxidase (POD) from rosemary. The sample was boiled in the presence of SDS and

2-mercaptoethanol, then separated on a 10% Laemmli gel. A calibration curve was used to determine the MW of the purified POD (log molecular weight of the standards vs. retention factor). 12% Sodium dodecyl sulfate-polyacrylamide gel electrophoresis (SDS-PAGE) was done according to Laemmli et al, as modified by Maizel [29,30]. It was used for protein localization, molecular mass estimation, and determination of the purity of the purified peroxidase (pooled, peak fractions from Matrex gel red A). Two methods were used to locate proteins or estimate purity: either by staining the gel with 0.1% (w/v) Coomassie brilliant blue R-250 or by running an unstained lane and cutting it horizontally to obtain 0.20 mm pieces, which were then suspended individually in buffer to detect peroxidase activity.

2.4.2. Effect of molecular mass on peroxidase

The molecular mass was calculated by using the relative migration distance (Rf) as stated by Maizel [30]. The standards obtained from Bio-Rad Co., Richmond, Calif.

2.4.3. Determination of isoelectric point (pI)

1 mL of the purified peroxidase was dialyzed against 2 × 2 L (1% glycine buffer) and layered into Isoelectric focusing gel (pH 3.5 to 9.5) polyacrylamide gels along with the standard markers obtained from Pharmacia Biotech, Uppsala, Sweden [31].

2.4.4. Optima pH and temperature

The optimum pH was determined by measuring pH at different values during purification of peroxidase activity. In contrast, the optimum temperature was measured at different temperatures within the same assay mixture in both cases. The optimal pH and temperature were 6.0 and 40°C, respectively

2.4.5. Km and Vmax values

The Km and Vmax values were determined from the Lineweaver-Burk graph using the method described by Hisar et al. [32]. The reaction mixture consists of 50 µL of the purified enzyme, 950 mL McIlvaine buffer, pH 6.0, and either a fixed

amount of 1 mL of hydrogen peroxide (H₂O₂, 22.5 mM) with various concentrations of guaiacol or vice versa (i.e., with multiple concentrations of guaiacol, 45 mM with different concentrations of hydrogen peroxide at 40°C). The kinetic data were analyzed and read at 480 nm [33].

2.5. Determination and effect of metals in Rosemary

The impact of several metal ions (calcium, cobalt, iron, magnesium, sodium, potassium, zinc) was studied using three concentrations in the assay mixture (2, 5, and 10 mM). The above metals were determined in rosemary after microwave digestion and by F-AAS (Fig. 1). The burner height was optimized for each element (typically 10–12 mm above the base on many instruments). Fuel flow instrument default for air-acetylene (~2.0 L min⁻¹). Lamp current (mA) and wavelength (nm) are used for each element-specific lamp and wavelength (Ca: 422.7 nm, Mg: 285.2 nm, Cu: 324.8 nm, Zn: 213.9 nm, Mn: 279.5 nm, Pb: 217.0 nm (or 283.3 nm), Cd: 228.8 nm, Ni: 232.0 nm). Digest 0.25–0.5 g powder in a closed-vessel microwave using concentrated 5 mL HNO₃ and 1.0 mL H₂O₂ (Ramp to 200 °C in 5 min, hold 15–20 min). After digestion in a microwave for 20 min, the mixture was diluted to 5 mL with DW. The solution is analyzed using flame AAS (air-acetylene) after establishing a calibration curve with standard solutions (mg kg⁻¹ or mg g⁻¹).

3. Results and Discussion

3.1. HPLC and F-AAS Results

Due to the HPLC-UV method, there was a statistically significant difference ($p < 0.05$) between the amount of total phenolic compounds extracted from the rosemary at different temperatures. HPLC analysis of phenolic compounds in rosemary includes 3,4,5-trihydroxybenzoic acid with a minimum retention time of 4.0 min, and cinnamic acid as a monocarboxylic acid (C₈H₉O₂), observed at a maximum retention time of 22.0 min with a concentration of 14.26 mg per 100 g of Rosemary (Fig. 2). Among all the detected compounds, the highest amount was pyrocatechol (8.5 min, C₆H₄(OH)₂) at

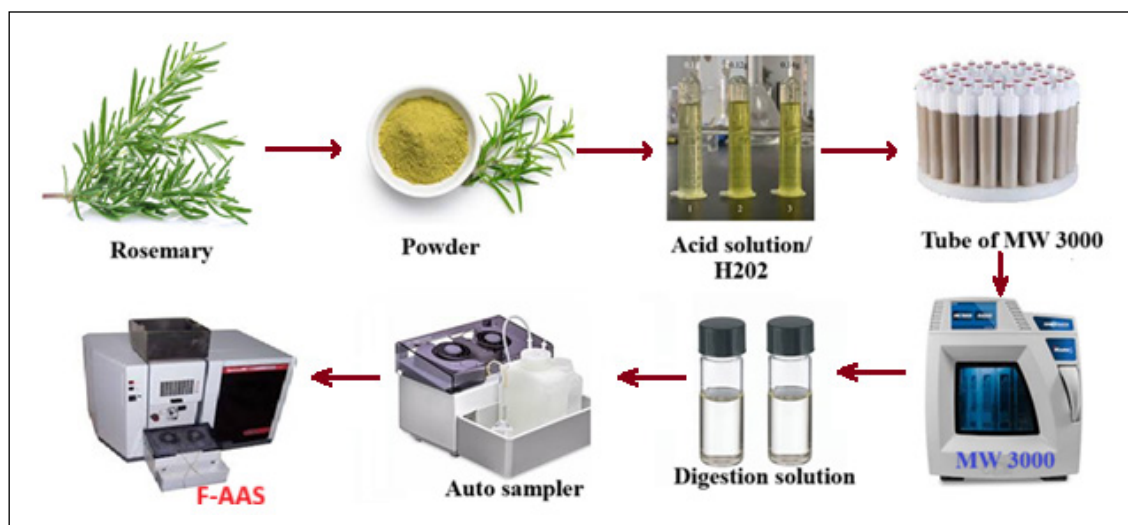


Fig. 1. Determination of metals in Rosmary by microwave digestion and F-AAS

1500 mg g⁻¹, while the lowest was 4-hydroxycinnamic acid (23 min) at 3.13 mg g⁻¹. Other compounds, such as 4-hydroxybenzoic acid (9.2 min), 4-hydroxy-3-methoxybenzoic acid (10.4 min), syringic acid as dimethoxybenzene (11.4 min), and 4-hydroxy-3-methoxybenzaldehyde (12.5 min), were identified with over 100 mg g⁻¹. The mineral composition of the rosemary extract, including sodium, potassium, calcium, phosphorus, magnesium, iron, copper, manganese, and zinc, was determined using Flame atomic absorption spectroscopy (FAAS). The mean concentration of elements in rosemary measured

by F-AAS was: sodium (Na) 91.23 mg per 100 g, potassium (K) 1956.29 mg per 100 g, calcium (Ca) 1078.58 mg per 100 g, phosphorus (P) 389.85 mg per 100 g, magnesium (Mg) 37.44 mg per 100 g, iron (Fe) 32.32 mg per 100 g, copper (Cu) 0.86 mg per 100 g, manganese (Mn) 5.52 mg per 100 g, and zinc (Zn) 9.23 mg per 100 g of rosemary.

3.2. Purification

An outline of various steps of the extraction and purification of a peroxidase from rosemary is given in [Table 1](#).

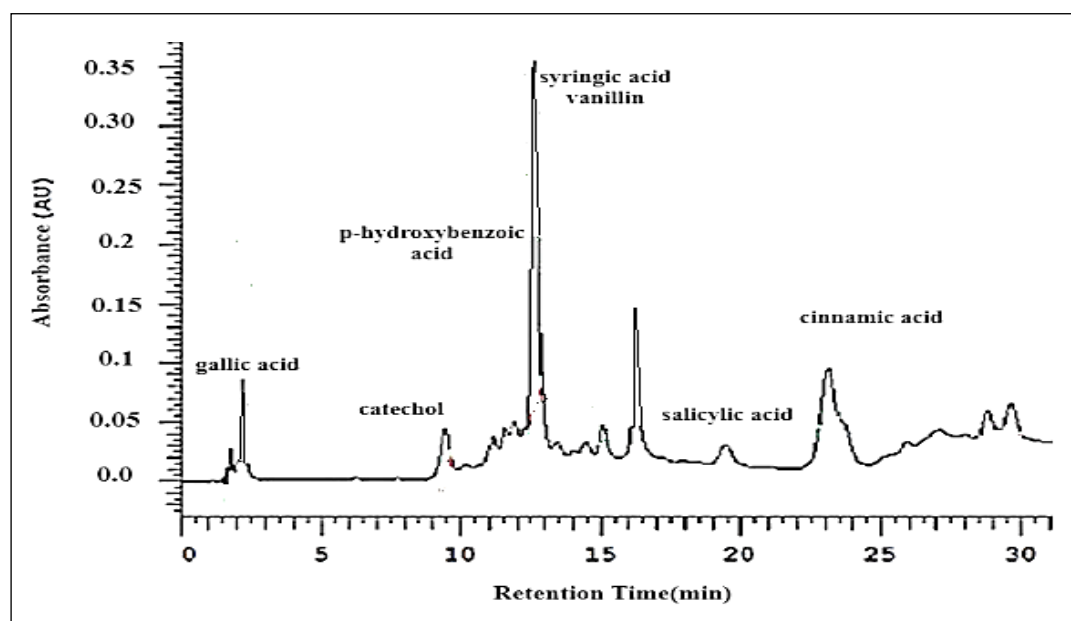


Fig.2. HPLC analysis of phenolic compounds in rosemary

Table 1. Purification steps of Rosemary's peroxidase

Fraction	Vol. (mL)	TPA (units)	TP (mg)	SA (units× mL ⁻¹)	Recovery (%)	Purification
Crude extract	400	4650	16270	0.20	100.00	1.00
0.6-0.8% (NH ₄) ₂ SO ₄	6	4322	2550	1.69	93.00	8.47
Phospho-cellulose	60	3611	343	10.52	77.65	52.63
DEAE-cellulose	40	2412	23	104.86	51.87	524.34
Sephadex G-100	24	2230	8	278.75	47.95	1393.75
Matrex gel red-A	6	1650	1.8	916.67	35.50	4583.35

TPA: Total Peroxidase activity, TP: Total protein, SA: Specific activity

The elution profile of a 0.6-0.8% (NH₄)₂SO₄ saturation fraction on a phosphocellulose column (Fig. 3a) shows that most of the peroxidase activity was eluted at a 0.31 M sodium chloride gradient. In contrast, small amounts of activity were scattered apparently through the elution volume.

When the pooled peak fractions from the first column were loaded into the DEAE-cellulose

column (Fig. 3b), there was no significant loss in peroxidase activity. Still, a considerable reduction in the protein content was obtained by using the two previous columns (Table 1). The third column (Sephadex G-100) was used primarily to remove the excess salt from the enzyme. The pooled peak fractions from the Matrix gel Red A column (Fig. 3c) were considered the purified enzyme.

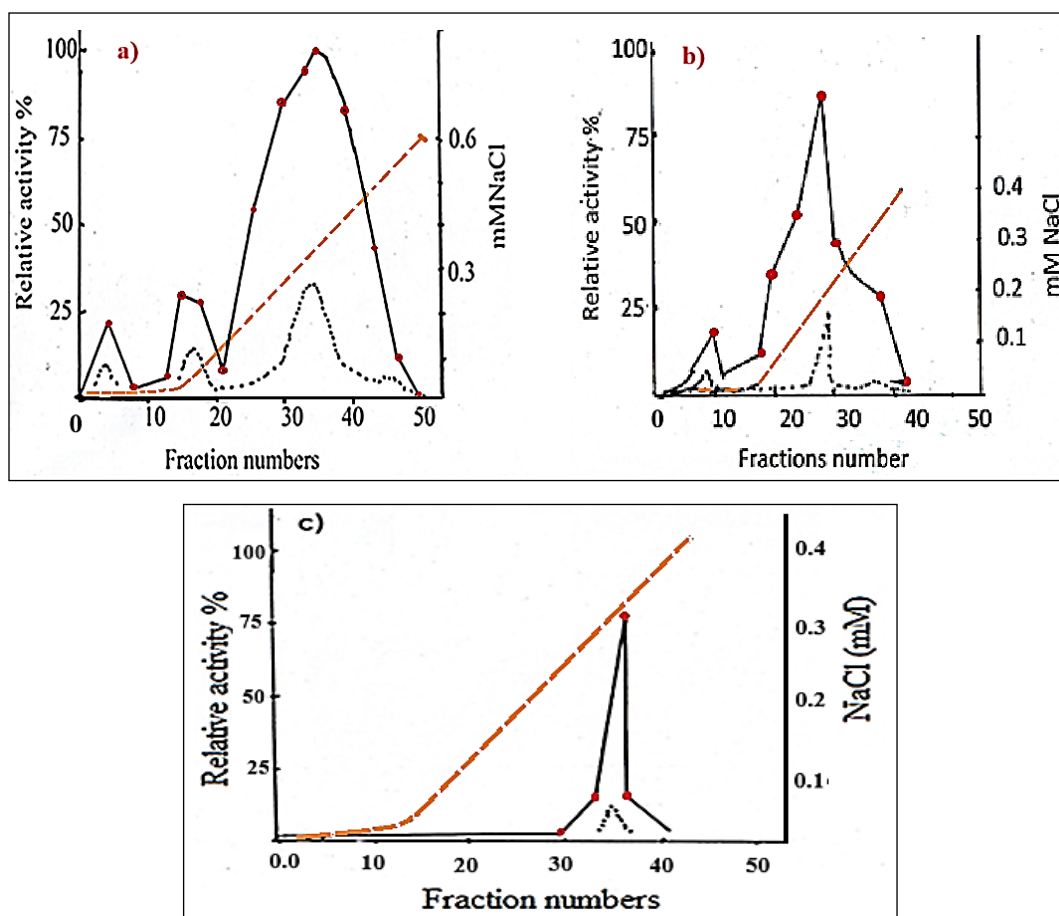


Fig.3. The elution profile of Rosemary's peroxidase activity, **a)** on Phosphocellulose column, **b)** DEAE-cellulose column, and **c)** on Matrix gel red A column

3.3. Determination of a molecular mass

The purified peroxidase was tested for purity and isozyme composition by SDS-PAGE. An evident band was observed at 47 kDa using a Bio-6000T gel scanner (BIOIMAGER) after staining. By analyzing 0.2 mL cut pieces of an unstained gel, it seems that most of the peroxidase activity is concentrated in the 47.0 kDa band. In contrast, minimal activity was in the positions of the 25 and 18 kDa bands (Fig. 4). So, a significant protein band was observed at approximately 47 kDa, corresponding to the dominant POD isoform. Activity staining of 0.2-mL gel slices confirmed that the majority of peroxidase activity was localized within the 47 kDa band, whereas only minimal activity was detected in the faint lower-molecular-weight bands at ~25 and ~18 kDa. This result indicates that the purified enzyme preparation predominantly contains a single active POD isoform

3.4. Determination of the Iso-electro focusing point (pI)

The enzyme has an isoelectric point (pI) of 4.33.

The pI of 4.33 indicates that the peroxidase becomes electrically neutral at acidic pH. Below pH 4.33, the enzyme carries a net positive charge, while above this pH, it becomes negatively charged. A pI in this range is typical for plant peroxidases and reflects the enzyme's acidic amino-acid composition and optimal solubility behavior.

3.5. Optimum pH and temperature

The effect of temperature was evaluated over the range of 25 °C to 80 °C. The results showed us that the optimal temperature is 40 °C. Additionally, the effect of pH on the purified peroxidase activity (PPA) from Rosemary was studied from pH 2 to 11. The results show that the highest purified peroxidase activity in Rosemary was observed at pH 6. Therefore, the purified peroxidase exhibits optimal activity at 40 °C and pH 6.0. (Fig. 5a and 5b). The two-panel schematic figure depicting the thermal stability of purified peroxidase from rosemary (activity vs. temperature and residual activity vs. incubation time at 40/50/60 °C), presented in Schema 3.

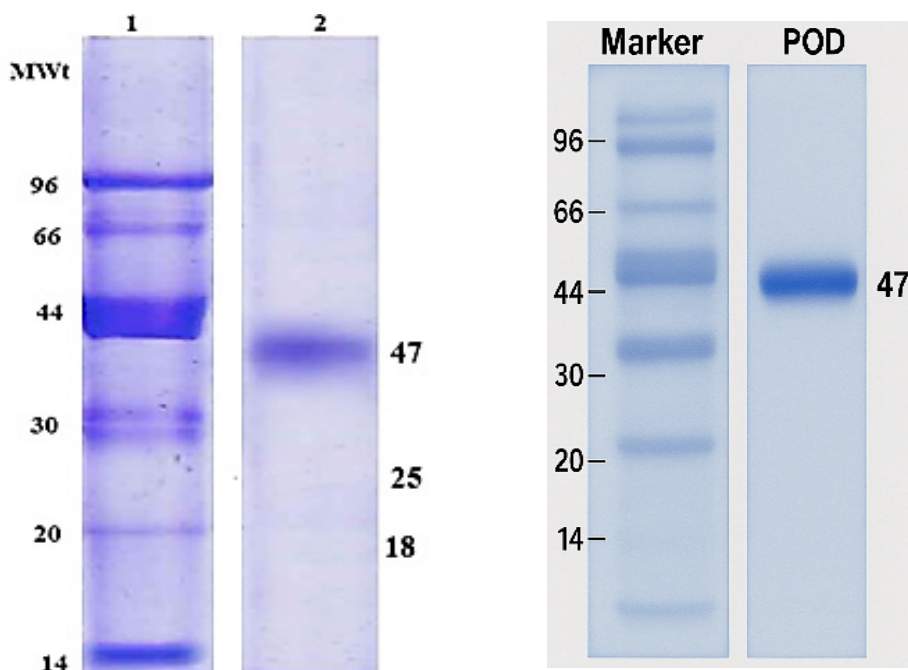


Fig. 4. SDS-PAGE for Rosemary's peroxidase with standard molecular markers (two bands of 25 and 18 kDa were very faint and could not be shown during staining).

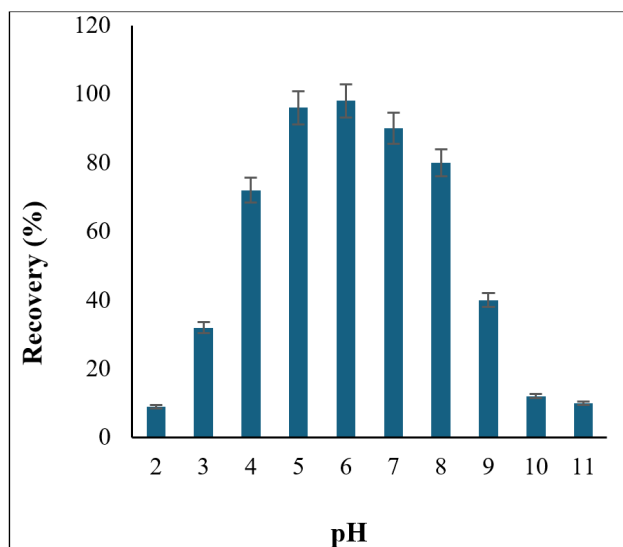


Fig. 5a. Effect of pH on PPA of Rosemary

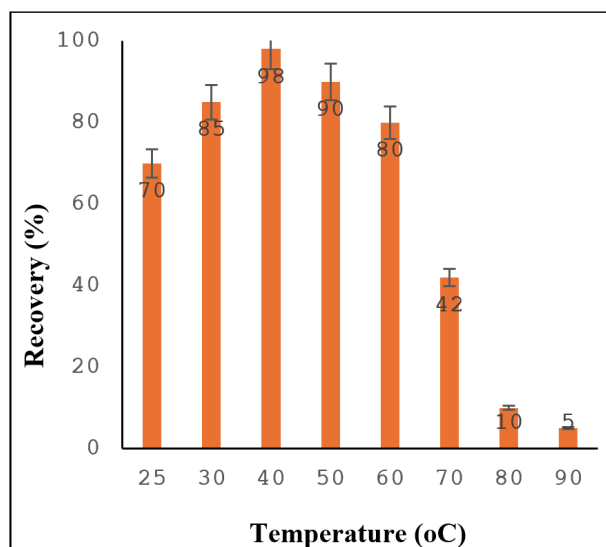
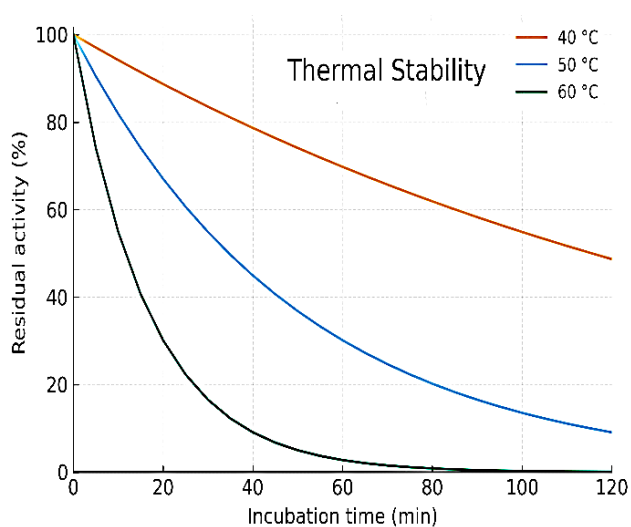
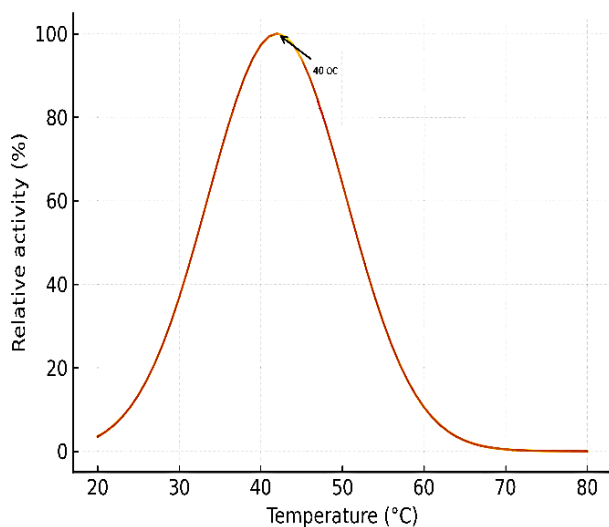


Fig. 5b. Effect of temperature on PPA of Rosemary



Schema 3. Thermal stability of purified rosemary peroxidase (leaf enzyme)

3.6. Determination of K_m and V_{max}

The K_m and V_{max} values of the purified peroxidase were measured from Lineweaver-Burk plots. The activities of the purified peroxidase were calculated at various concentrations of guaiacol substrate. In contrast, the concentration of hydrogen peroxide was stable (Fig. 6a) and the other way around (Fig. 6b), where various hydrogen peroxide

concentrations were measured while guaiacol remained stable at 40 °C. K_m and V_{max} values were 21.3 and 33.1 mM and 0.19 and 0.87 mM, respectively. K_{cat} values were 577 S^{-1} and 1528 S^{-1} , respectively, while the efficiency constant (K_{cat}/K_m) was 27.8 and 46.2 for guaiacol and hydrogen peroxide, respectively.

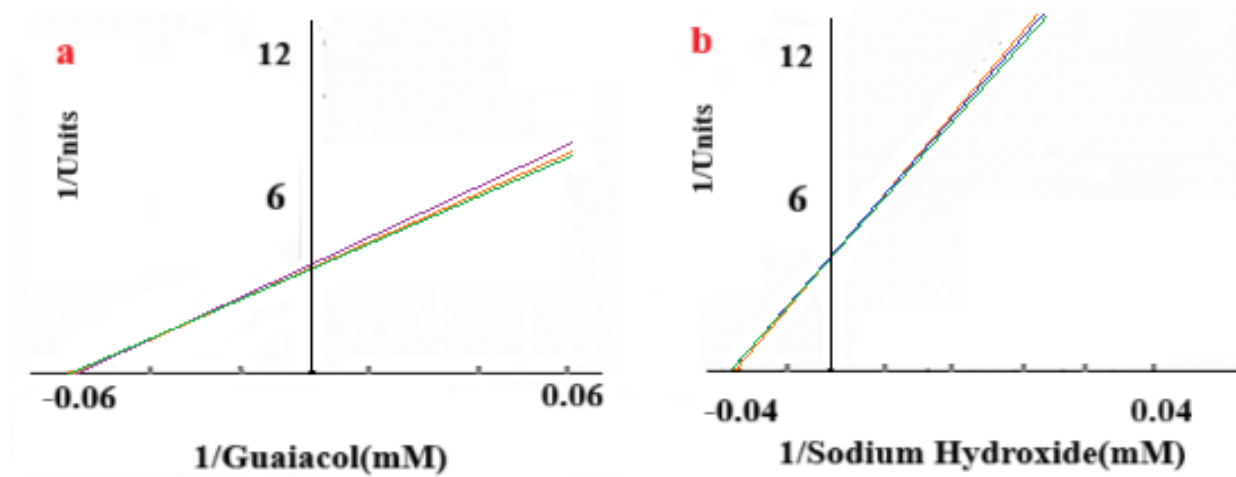


Fig. 6. Lineweaver–Burk plot and Substrate saturation curve of Rosemary's peroxidase activity in the presence of (a) guaiacol and (b) H_2O_2 concentrations as a fixed substrate.

3.7. Effects of metal ions

Rosemary's purified peroxidase was enhanced with calcium, ferric, magnesium, and manganese ions. Aluminum, cobalt, nickel, sodium, and potassium ions do not affect the enzyme, whereas copper, mercury, and zinc ions inhibit it significantly (Table 2).

3.8. Discussion

The results showed that peroxidase was successfully purified from Rosemary, with 40% recovery. Peroxidase activity is concentrated in a single band (47.0 kDa) that is easily visible on the

stained gel. Two very faint 25.0-kDa and 18.0-kDa bands, barely visible but detectable in the cut pieces of the gel, suggest that the enzyme is composed of three polypeptide chains linked by disulfide bonds. Most purified peroxidases consist of a single polypeptide chain around 40-50 kDa, such as *gingers* and *Panaeolus' peroxidase* of 42 kDa [34,35], *horseradish's* 40 kDa [36], *chickpeas* 39 kDa [37]. The peroxidase from a fresh cauliflower bud has a molecular weight of 44 kDa [38]. *J. curcas* leaves have a peroxidase with a molecular mass of 48 kDa [39]. Other researchers, such as Scialabba et al. [40], have reported the presence

Table 2. Effects of some metal ions on the purified peroxidase enzyme

Metal ions	Relative activity (%)		
	2.0 mM	5.0 mM	10 mM
Al^{3+}	100	95	95
Ca^{2+}	350	370	370
Co^{2+}	100	95	99
Cu^{2+}	23	0	0
Fe^{3+}	322	352	382
Hg^{2+}	20	0	0
K^{1+}	100	98	100
Mg^{2+}	350	360	360
Mn^{2+}	270	270	270
Na^{1+}	98	98	96
Ni	100	100	100
Pb	0	0	0
Zn^{2+}	0	0	0

of a peroxidase in maturing radish seeds, which is composed of four isozymes with molecular masses of 98, 52.5, 32.8, and 29.5 kDa, respectively. The optimum pH for any enzyme depends on its environment of operation, typically in the cell, and varies according to the enzyme-substrate type. In contrast, the optimum temperature for any enzyme depends upon its structure and its amino acid composition. The results showed that Rosemary's purified peroxidase has an optimum pH of 6.0 and a temperature of 40°C, which is compatible with that of *Solanum ethiopicum* L. (white) peroxidase [41] and that of *C. reticulata* [42]. In general, several researchers stated that most plant peroxidases have an optimal pH and temperature of (6-7) and (40-50 °C), respectively [13, 39, 43, 44]. In some cases, the optimum temperature can reach 60°C, for example, in both *date palm cv. Agwa's peroxidase* [45, 30]. Some researchers have shown that peroxidases with low optimum temperatures (30 °C and 10 °C) are present in purified peroxidases from buckwheat seeds [46]. The K_m and V_{max} kinetic values of the purified Rosemary peroxidase for its substrates guaiacol and hydrogen peroxide were compared with similar values from different extracted peroxidases. The K_m values for peroxidase from Arabian balsam stems are 46.5 mM for guaiacol and 4.81 mM for hydrogen peroxide. In contrast, those for horseradish peroxidase are 32.36 mM for guaiacol and 5.86 mM for hydrogen peroxide, respectively [47]. In *R. sativus*, K_m values of 0.036 ± 0.08 mM and 0.0084 ± 0.003 mM for guaiacol and hydrogen peroxide substrates, respectively, while V_{max} was 0.138 EU/mol/min for *o*-dianisidine and 0.032 EU/min for hydrogen peroxide, respectively [48,49]. This comparison suggests that *Rosemary's peroxidase* has a higher affinity for guaiacol than for hydrogen peroxide. The activity of the purified peroxidase from Rosemary was intensified in the presence of calcium, ferric, magnesium, and manganese ions, which were compatible with other purified peroxidases [9, 4, 6]. Additionally, a gas chromatography flame ionization detector (GC-FID) or gas chromatography mass spectrometry (GC-MS) is employed to identify polypeptide

chains of approximately 40-50 kDa by analyzing volatile amino acid derivatives, typically after hydrolyzing the polypeptide into smaller peptides or amino acids. Many previous articles used GC-FID or GC-MS for the determination of organic material [20, 24, 25, 50-55]. Calcium ions seem to maintain the conformation of some proteins in this enzyme. In contrast, both magnesium and manganese ions play crucial roles in the catalytic process of photosynthesis and the release of oxygen. Ferric ions participate in the peroxidase-oxidase cycle, and, surprisingly, only Shank et al. reported that ferric ions inhibit the peroxidase purified from finger roots. The metal ions: aluminum, cobalt, nickel, potassium, and sodium did not affect the activity of the purified peroxidase, but Nouren et al. showed that the mentioned metal ions intensified *C. reticulata* peels' peroxidase activity [42]. Khatum et al. reported that some metal ions, such as aluminum, cadmium, copper, magnesium, nickel, phosphorus, and zinc ions, showed minimal inhibitory effects, while ferric and ferrous ions, along with mercury ions, exhibited a maximum inhibitory effect on *M. oleifera* L. leaves' peroxidase [49]. Copper, mercury, phosphorus, and zinc ions inhibited purified peroxidases as well as many extracted peroxidases [13, 48, 2, 30, 35]. These inhibitors presumably bind to the enzyme's active-site SH groups, leading to irreversible inhibition.

4. Conclusions

Rosemary is readily available in large quantities year-round and can be readily used to produce peroxidases for various applications, including biochemistry, biotechnology, the food industry, wastewater treatment, and other industrial processes. Rosemary's peroxidase has a similar molecular weight and chemical properties to other Class III plant peroxidases studied previously, but it achieves a 35% recovery after purification and remains stable across broad pH and temperature ranges, specifically between pH 4-7 and 30-60°C, for an extended period. This stability offers an advantage for its industrial applications. Rosemary's

peroxidase was purified by chromatographic techniques and analyzed by F-AAS and HPLC. The LOD and LOQ of the HPLC method were determined at 0.044-0.058 $\mu\text{g mL}^{-1}$ and 0.147-0.159 $\mu\text{g mL}^{-1}$, respectively.

5. Acknowledgement

There is no interest in financial profits or any conflict of interest related to this work, as stated in this research paper, due to the knowledge of the authors.

6. References

- [1] D. Kregiel, E. Pawlikowska, H. Antolak, *Urtica* spp.: Ordinary plants with extraordinary properties, *Molecules*, 23 (2018) 1664. <https://doi.org/10.3390/molecules23071664>
- [2] B. Jiang, D. Duan, L. Gao, Properties and applications of plant peroxidases, *J. Biochem. Technol.*, 15 (2024) 3-8. <https://doi.org/10.51847/6C0QKTK3Na>
- [3] S. Yang, Q.-L. Gao, Obtaining peroxidase from *Zanthoxylum armatum* DC, fruit, and application in detoxification of phenol wastewater, *Ind. Crops Prod.*, 193 (2023) 116265. <https://doi.org/10.1016/j.indcrop.2023.116265>
- [4] F. Topal, M. Nar, H. Gocer, P. Kalin, U. M. Kocyigit, İ. Gülçin, S. H. Alwasel, Antioxidant activity of taxifolin: an activity-structure relationship, *J. Enzyme Inhib. Med. Chem.*, 31 (2016) 674-83. <https://doi.org/10.3109/14756366.2015.1057723>
- [5] P. P. Galende, C. G. de María, J. B. Arellano, M. G. Roig, Va. L. Shnyrov, Study on extraction, purification and characterization of a novel peroxidase from white Spanish Broom (*Cytisus Multiflorus*), *Int. J. Plant Biol. Res.*, 4 (2016) 1052. <https://www.jscimedcentral.com/public/assets/articles/plantbiology-4-1052.pdf>
- [6] M. M. S. Julião, S.T. Oliveira, L.B.S. Andrade, M.F. Figueiredo, H.O. Salles, Partial purification and thermal stability of two peroxidases from *Pithecellobium dulce* (Roxb.) benth. aril, *Rev. Virtual Quim.*, 8 (2016) 1913-1923. <https://doi.org/10.21577/1984-6835.20160130>
- [7] S. A. Mohamed, M. H. Al-Harbi, Y. Q. Almulaiky, I.H. Ibrahim, R. M. El-Shishtawy, Immobilization of horseradish peroxidase on Fe_3O_4 magnetic nanoparticles, *Electron J. Biotechnol.*, 27 (2017) 84–90. <https://doi.org/10.1016/j.ejbt.2017.03.010>
- [8] D.A. Centeno, X.H. Solano, J.J. Castillo, A new peroxidase from leaves of guinea grass (*Panicum maximum*): A potential biocatalyst to build amperometric biosensors, *Bioelectrochemistry*, 116 (2017) 33–38. <https://doi.org/10.1016/j.bioelechem.2017.03.005>
- [9] A. Oztekin, Z. Almaz, S. Gerni, D. Erel, S.M. Kocak, M.E. Sengül, H. Ozdemir, Purification of peroxidase enzyme from radish species in fast and high yield with affinity chromatography technique, *J. Chromatogr. B*, 1114–1115 (2019) 86–92. <https://doi.org/10.1016/j.jchromb.2019.03.035>
- [10] M. Hamid, K. Rehman, Potential applications of peroxidases, *Food Chem.*, 115 (2009) 1177–1186. <https://doi.org/10.1016/j.foodchem.2009.02.035>
- [11] U. Kalsoom, S.S. Ashraf, M.A. Meetani, M.A. Rauf, H.N. Bhatti, Mechanistic study of a diazo dye degradation by soybean peroxidase, *Chem. Cent. J.*, 7 (2013) 93. <https://doi.org/10.1186/1752-153X-7-93>
- [12] A.C. Osuji, S.O. Eze, E.E. Osayi, F.C. Chilaka, Biobleaching of industrial important dyes with peroxidase partially purified from garlic, *Sci. World J.*, 2014 (2014) 183163. <https://doi.org/10.1155/2014/183163>
- [13] B.M. Majeke, F.X. Collard, L. Tyhoda, J.F. Görgens, The synergistic application of quinone reductase and lignin peroxidase for the deconstruction of industrial (technical) lignins and analysis of the degraded lignin products, *Bioresour. Technol.*, 319 (2021) 124152. <https://doi.org/10.1016/j.biortech.2020.124152>
- [14] M. Ayala, J. Verdín, R. Vazquez-Duhalt, The

- prospects for peroxidase-based biorefining of petroleum fuels, *Biocatal. Biotransform.*, 25 (2007) 114–129.
<https://doi.org/10.1080/10242420701379015>
- [15] A. Rashidi, A. Vahid, Arsenic speciation based on amine-functionalized bimodal mesoporous silica nanoparticles by ultrasound assisted-dispersive solid-liquid multiple phase microextraction, *Microchem. J.*, 130 (2017) 137-146.
<https://doi.org/10.1016/j.microc.2016.08.013>
- [16] N. Esmaili, J. Rakhtshah, Ultrasound assisted-dispersive-modification solid-phase extraction using task-specific ionic liquid immobilized on multiwall carbon nanotubes for speciation and determination mercury in water samples, *Microchem. J.*, 154 (2020) 104632.
<https://doi.org/10.1016/j.microc.2020.104632>
- [17] M. K. Abbasabadi, F. Hosseini, Nanographene oxide modified phenyl methanethiol nanomagnetic composite for rapid separation of aluminum in wastewaters, foods, and vegetable samples by microwave dispersive, *Food Chem.*, 347 (2021) 129042.
<https://doi.org/10.1016/j.foodchem.2021.129042>
- [18] M. Arjomandi, A review: analytical methods for heavy metals determination in environment and human samples, *Anal. Methods Environ. Chem. J.*, 2 (2019) 97-126.
<https://doi.org/10.24200/amecj.v2.i03.73>
- [19] J. Rakhtshah, M. Dehghani Mobarake, Simultaneously speciation and determination of manganese (II) and (VII) ions in water, food, and vegetable samples based on immobilization of N-acetylcysteine on multi-walled carbon nanotubes, *Food Chem.*, 389 (2022) 133124.
<https://doi.org/10.1016/j.foodchem.2022.133124>
- [20] J. Rakhtshah, N. Esmail, A rapid extraction of toxic styrene from water and wastewater samples based on hydroxyethyl methylimidazolium tetrafluoroborate immobilized on MWCNTs by ultra-assisted dispersive cyclic conjugation-micro-solid phase extraction, *Microchem. J.*, 170 (2021) 106759.
<https://doi.org/10.1016/j.microc.2021.106759>
- [21] M. D. Mobarake, Ultrasound-assisted solid-liquid trap phase extraction based on functionalized multi-wall carbon nanotubes for preconcentration and separation of nickel in petrochemical waste water, *J. Anal. Chem.*, 74 (2019) 865-876.
<https://doi.org/10.1134/S1061934819090090>
- [22] A. F. Zarandi, An immobilization of 2-(Aminomethyl) thiazole on MWCNTs used for rapid extraction of manganese ions in hepatic patients, *J. Pharm. Biomed. Anal.*, 240 (2024) 115941.
<https://doi.org/10.1016/j.jpba.2023.115941>
- [23] M. K. Abbasabadi, Speciation of cadmium in human blood samples based on Fe₃O₄-supported naphthalene-1-thiol- functionalized graphene oxide nanocomposite by ultrasound-assisted dispersive magnetic micro solid phase extraction, *J. Pharm. Biomed. Anal.*, 189 (2020) 113455.
<https://doi.org/10.1016/j.jpba.2020.113455>
- [24] S. Teimoori, An immobilization of aminopropyl trimethoxysilane-phenanthrene carbaldehyde on graphene oxide for toluene extraction and separation in water samples, *Chemosphere*, 316 (2023) 137800.
<https://doi.org/10.1016/j.chemosphere.2023.137800>
- [25] S. Teimoori, A. H. Hassani, M. Panahi, N. Mansouri, Rapid extraction of BTEX in water and milk samples based on functionalized MWCNTs by dispersive homogenized-micro-solid phase extraction, *Food Chem.*, 421 (2023) 136229.
<https://doi.org/10.1016/j.foodchem.2023.136229>
- [26] B. Aydın, I. Gülçin, S. Alwasel, Purification and characterization of polyphenol oxidase from Hemşin apple (*Malus communis* L.), *Int. J. Food Prop.*, 18 (2015) 2735-2745.
<https://doi.org/10.1080/10942912.2015.1012725>
- [27] I. Gülçin, Antioxidant activity of cauliflower (*Brassica oleracea* L.), *Turk. J. Agric. For.*, 32 (2008) 65–78.
<https://journals.tubitak.gov.tr/agriculture/vol32/iss1/8/>
- [28] O.H. Lowry, N.J. Rosebrough, A.L. Farr, R.J.

- Randall, Protein measurement with the Folin phenol reagent, *J. Biol. Chem.*, 193 (1951) 265–275.
[https://www.jbc.org/article/S0021-9258\(19\)52451-6/pdf](https://www.jbc.org/article/S0021-9258(19)52451-6/pdf)
- [29] U.K. Laemmli, Cleavage of structural proteins during the assembly of the head of bacteriophage T4, *Nature*, 227 (1970) 680–685.
<https://doi.org/10.1038/227680a0>
- [30] J.V. Maizel, SDS polyacrylamide gel electrophoresis, *Trends Biochem. Sci.*, 25 (2000) 590–592.
[https://doi.org/10.1016/s0968-0004\(00\)01693-5](https://doi.org/10.1016/s0968-0004(00)01693-5)
- [31] O. Vesterberg, H. Svensson, Isoelectric fractionation, analysis and characterization of ampholytes in natural pH gradients. IV. Further studies on the resolving power in connection with separation of myoglobins, *Acta Chem. Scand.*, 20 (1966) 820–834.
<https://doi.org/10.3891/acta.chem.scand.20-0820>
- [32] H. Lineweaver, D. Burk, The determination of enzyme dissociation constants, *J. Am. Chem. Soc.*, 56 (1934) 658–666.
<https://doi.org/10.1021/ja01318a036>
- [33] A. Yıldırım, U. Atmaca, A. Keskin, M. Topal, M. Çelik, İ. Gülçin, C.T. Supuran, N-Acylsulfonamides strongly inhibit human carbonic anhydrase isoenzymes I and II, *Bioorg. Med. Chem.*, 23 (2015) 2598–2605.
<https://doi.org/10.1016/j.bmc.2014.12.054>
- [34] S.A. Mohamed, M.O. El-Badry, E.A. Drees, A.S. Fahmy, Properties of a cationic peroxidase from *Citrus jambhiri* cv. Adalia, *Appl. Biochem. Biotechnol.*, 150 (2008) 127–137.
<https://doi.org/10.1007/s12010-008-8142-2>
- [35] M. Heinzkill, L. Bech, T. Halkier, P. Schneider, T. Anke, Characterization of laccases and peroxidases from wood-rotting fungi (family Coprinaceae), *Appl. Environ. Microbiol.*, 64 (1998) 1601–1606.
<https://doi.org/10.1128/aem.64.5.1601-1606.1998>
- [36] C.B. Lavery, M. C. Macinnis, M. J. Macdonald, J. B. Williams, C. A. Spencer, A. A. Burke, D. J. Irwin, G. B. D’Cunha, Purification of peroxidase from horseradish (*Armoracia rusticana*) roots, *J. Agric. Food Chem.*, 58 (2010) 8471–8476.
<https://doi.org/10.1021/jf100786h>
- [37] H. Bhatti, U. Kalsoom, A. Habib, Decolorization of direct dyes using peroxidase from *Raphanus sativus*, *J. Chem. Soc. Pak.*, 34 (2012) 257–262.
<https://jcspp.org.pk/ArticleUpload/4143-20043-1-CE.pdf>
- [38] H.Ü. Erdem, R. Kalın, N. Özdemir, H. Özdemir, Purification and biochemical characterization of peroxidase isolated from white cabbage (*Brassica oleracea* var. capitata f. alba), *Int. J. Food Prop.*, 18 (2015) 2099–2109.
<https://doi.org/10.1080/10942912.2014.963868>
- [39] F. Cai, C. Ouyang, P. Duan, S. Gao, Y. Xu, F. Chen, Purification and characterization of a novel thermally stable peroxidase from *Jatropha curcas* leaves, *J. Mol. Catal. B: Enzym.*, 77 (2012) 59–66.
<https://doi.org/10.1016/j.molcatb.2011.12.002>
- [40] A. Scialabba, L. Bellani, Effects of ageing on peroxidase activity and localization in radish (*Raphanus sativus* L.) seeds, *Eur. J. Histochem.*, 46 (2002) 351–358.
<https://doi.org/10.4081/1747>
- [41] S. A. H. Mirzahosseini, S. A. Moussavi-Najarkola, H. Farahani, the evaluation and determination of heavy metals pollution in edible vegetables, water, and soil in the south of Tehran province by GIS, *Arch. Environ. Prot.*, 41 (2015) 63–72.
<https://doi.org/10.1515/aep-2015-0020>
- [42] S. Nouren, H. Bhatti, I. Bhatti, M. Asgher, Kinetic and thermal characterization of Peroxidase from peels of *Citrus reticulata* var. Kinnow, *J. Anim. Plant Sci.*, 23 (2013) 430–435.
<https://thejaps.org.pk/docs/v-23-2/17.pdf>
- [43] D. Borah, S. Shah, R. Yadav, Extraction and characterization of peroxidase from *Camellia sinensis*, *Proc. Natl. Acad. Sci. India Sect. B: Biol. Sci.*, 84 (2014) 343–348.
<https://doi.org/10.1007/s40011-013-0211-9>

- [44] B. Somtürk, R. Kalın, N. Özdemir, Purification of peroxidase from red cabbage (*Brassica oleracea* var. *capitata* f. *rubra*) by affinity chromatography, *Appl. Biochem. Biotechnol.*, 173 (2014) 1815–1828.
<https://doi.org/10.1007/s12010-014-0968-1>
- [45] M. Zeyadi, Purification and characterization of peroxidase from date palm cv. Agwa fruits, *Int. J. Food Prop.*, 22 (2019) 1910–1919.
<https://doi.org/10.1080/10942912.2019.1691589>
- [46] T. Suzuki, Y. Honda, Y. Mukasa, S.J. Kim, Characterization of peroxidase in buckwheat seed, *Phytochem.*, 67 (2006) 219–224.
<https://doi.org/10.1016/j.phytochem.2005.11.014>
- [47] M. Şişecioglu, I. Gülçin, M. Çankaya, A. Atasever, H. Kaya, H. Özdemir, Purification and characterization of peroxidase from Turkish black radish (*Raphanus sativus* L.), *J. Med. Plant. Res.*, 4 (2010) 1187–1196.
<http://www.academicjournals.org/JMPR>
- [48] N.I. Ridzuan, N. Abdullah, Y.L. Vun, C.V. Supramaniam, Micropropagation and defence enzymes assessment of *Moringa oleifera* L. plantlets using nodal segments as explant, *S. Afr. J. Bot.*, 129 (2020) 56–61.
<https://doi.org/10.1016/j.sajb.2018.12.010>
- [49] K. Shahanaz, M.A. Ashraduzzaman, M.R. Karim, F. Pervin, N. Absar, A. Rosma, Purification and characterization of peroxidase from *Moringa oleifera* L. leaves, *Bioresources*, 7 (2012) 3237–3251.
<https://doi.org/10.15376/biores.7.3.3237-3251>
- [50] R. Ashouri, N. Mansouri, Dynamic and static removal of benzene from air based on task-specific ionic liquid coated on MWCNTs by sorbent tube-headspace solid-phase extraction procedure, *Int. J. Environ. Sci. Technol.*, 18 (2021) 2377–2390.
<https://doi.org/10.1007/s13762-020-02995-4>
- [51] R. Ashouri, S. A. Hajiseyed Mirzahosseini, N. Mansouri, Synthesis of carbon quantum Dots from olive stones for efficient adsorption of benzene from the ambient air, *J. Nanostruct.*, 11 (2021) 480–497.
<https://doi.org/10.22052/JNS.2021.03.007>
- [52] M. Mohammadi Asl, N. Mansouri, S. A. R. Haji Seyed Mirzahosseini, F. Atabi, Simultaneity comparative evaluation of toluene removal from the air by adsorption and UV semi-degradation-based adsorption procedure, *Int. J. Environ. Sci. Technol.*, 21 (2024) 6677–6694.
<https://doi.org/10.1007/s13762-024-05503-0>
- [53] M. Mohammadi Asl, F. Atabi, Functionalized graphene oxide with bismuth and titanium oxide nanoparticles for efficiently removing formaldehyde from the air by photocatalytic degradation–adsorption process, *J. Anal. Test.*, 7 (2023) 444–458.
<https://doi.org/10.1007/s41664-023-00272-0>
- [54] A. Faghihi-Zarandi, J. Rakhtshah, B. B. Yarahmadi, A rapid removal of xylene vapor from environmental air based on bismuth oxide coupled to heterogeneous graphene/graphene oxide by UV photo-catalectic degradation-adsorption procedure, *J. Environ. Chem. Eng.*, 8 (2020) 104193.
<https://doi.org/10.1016/j.jece.2020.104193>
- [55] C. D. T. Freitas, J. H Costa, Class III plant peroxidases: From classification to physiological functions, *Int. J. Biol. Macromol.*, 263 (2024) 130306.
<https://doi.org/10.1016/j.ijbiomac.2024.130306>